# Chapter 12 Spatial Distribution of Acoustic Radiation Force for Non-Contact Modal Excitation

Thomas M. Huber, Mikaela Algren, and Cole Raisbeck

Abstract In modal testing, a common excitation method is a transducer in mechanical contact with the object under test. However, for some structures it is desirable to excite vibrations without physical contact. One promising excitation technique is the acoustic radiation force. However, a challenge in using this technique is that the acoustic radiation force is spread out over a finite-diameter focal region. We describe a method to directly measure the spatial distribution of this force. An ultrasound transducer emitted sine waves with frequencies of, for example  $f_1 = 600.610$  kHz and  $f_2 = 600$  kHz; the resulting radiation force had a component at the difference frequency  $f_1$ - $f_2 = 610$  Hz. A MicroAcoustic Instruments BAT6 ultrasound transducer was focused to an approximately 2 mm diameter spot on a 19.6 by 8.1 by 0.37 mm clamped-free brass cantilever with a 610 Hz fundamental frequency. A vibrometer measured the response as this focus spot traversed the edge of the cantilever. This enabled determination of the distribution of the acoustic radiation force being delivered by the transducer. This may be helpful in future studies that involve modeling the force applied to a structure using the acoustic radiation force.

Keywords Ultrasound • Radiation force • Line-spread function • Vibrometer • Cantilever

#### 12.1 Introduction

In modal testing of small objects, one challenge can be to excite the vibrational modes without distortions due to mass loading. Using a laser Doppler vibrometer, it is relatively straightforward to measure the vibration in a non-contact manner; however, it is not always possible to excite these vibrations without contact. The ultrasound radiation force is a non-contact method of excitation resulting from insonifying a structure with a pair of ultrasound frequencies. The frequency difference is adjusted to the resonance frequency of the structure. Previous studies have demonstrated that this technique can be used in modal testing in air for structures as small as microcantilevers [1] to as large as the face of a classical guitar [2]. These previous studies demonstrated the feasibility of determining resonance frequencies of structures and also operating deflection shapes using a laser Doppler vibrometer. They, did not, however, quantify the magnitude or distribution of the applied radiation force.

The current study focused on using the ultrasound radiation force applied to a cantilever to directly measure the edge-spread function for an ultrasound transducer. Similar to its definition in optics, the edge-spread function is a measure of the integrated force distribution for a sharp-edged section of the circular ultrasound focus point. This was determined by translating the ultrasound focus point across the edge of a cantilever and monitoring the resulting radiation force using a single-point vibrometer. The line-spread function was the determined by numerical differentiation. The technique described is unique in that it enables measurement of the distribution of acoustic radiation force without the requirement of calibrated ultrasonic pressure measurement transducers.

## 12.2 Theory

### 12.2.1 Acoustic Radiation Force

Previous papers have described in detail the mechanism for ultrasound stimulated audio-range excitation, both in air [3] and in water [4, 5]. If an object is insonified with a pair of ultrasound frequencies,  $f_1$  and  $f_2$ , interference between the two frequencies produces a radiation force that results in a vibration of the object at the difference frequency  $\Delta f = f_2 - f_1$ . Both frequency components were emitted from a single transducer using a double-sideband suppressed-carrier amplitude modulated (AM) waveform [6]. The fundamental mode of a cantilever was excited using a difference frequency  $\Delta f$  by a transducer emitting two different ultrasound frequencies,  $f_1 = f_c - \Delta f/2$  and  $f_2 = f_c + \Delta f/2$ , symmetric about a central frequency  $f_c$ . Previous studies have shown that this radiation force can be used for modal excitation of a variety of systems [7–9].

As shown in Ref. [10], the acoustic radiation force on the object, in this case a cantilever, is proportional to the square of the acoustic pressure  $p(\mathbf{r},t)$  on the object. In particular, for a section of an object of area dS with drag coefficient  $d_r(\mathbf{r})$ , the acoustic radiation force would be given by [5]

$$F(\mathbf{r},t) dS = p(\mathbf{r},t)^2 / \rho c^2 d_r(\mathbf{r}) dS.$$
(12.1)

As described above, for the current experiment, the total pressure field is a double-sideband suppressed-carrier waveform with frequencies of  $f_1$  and  $f_2$ . This results in a total acoustic pressure

$$p(\mathbf{r}, t) = P(f_1, \mathbf{r}) \cos [2\pi f_1 t + \varphi_1(\mathbf{r})] + P(f_2, \mathbf{r}) \cos [2\pi f_2 t + \varphi_2(\mathbf{r})]$$
(12.2)

where P(f, r) is spatial distribution of the incident pressure field at frequency f. The phase differences  $\varphi_1(r)$  and  $\varphi_2(r)$  result from the waves of different frequencies traversing the distance between the transducer and the arrival point r.

The acoustic radiation force, with its dependence on the square of the acoustic pressure, will have a time-independent component, a component at the difference frequency  $\Delta f = f_2 - f_1$ , and high-frequency components at  $2f_1$ ,  $2f_2$ , and  $f_1 + f_2$ . In the current experiment, the pair of frequencies were adjusted so that the difference frequency corresponded to the cantilever's 610 Hz resonance frequency when the central frequency of the transducer was about 600 kHz. This means that the high-frequency components were far beyond the resonance frequency of the cantilever, and thus did not produce a measurable excitation. Also, because the two frequencies  $f_1$  and  $f_2$  differ by less than 0.1 %, the phase of both frequency components can be considered equal  $\varphi_1(\mathbf{r}) = \varphi_2(\mathbf{r})$ . This results in an acoustic radiation force at frequency  $\Delta f$  that can be written as

 $F_{\Delta f}(\mathbf{r}) \cos(2\pi t \Delta f)$  where the magnitude of the radiation force is

$$F_{\Delta f}(\mathbf{r}) = P(f_1, \mathbf{r}) P(f_2, \mathbf{r}) / \rho c^2.$$
(12.3)

The total magnitude of the acoustic radiation force on a surface S can thus be written as the surface integral

$$F_{S} = \iint_{S} F_{\Delta f}(\mathbf{r}) \ d_{r}(\mathbf{r}) dS = \frac{1}{\rho c^{2}} \iint_{S} P(f_{1}, \mathbf{r}) \ P(f_{2}, \mathbf{r}) \ d_{r}(\mathbf{r}) dS. \tag{12.4}$$

In the case where the drag coefficient  $d_r(\mathbf{r})$  is essentially constant over the ultrasound focus region, such as the current case where the target is a cantilever [11], and the focus region is much smaller than the size of the cantilever, the drag term can be taken outside of the integral, resulting in an acoustic radiation force

$$F_{S} = k \iint_{S} P(f_{1}, \mathbf{r}) P(f_{2}, \mathbf{r}) dS.$$
 (12.5)

where k is a constant that depends on the target geometry, drag force, and other constants.

To eliminate standing waves between the transducer and surface, the frequencies  $f_1$  and  $f_2$  were rapidly varied using a random carrier packet algorithm [12] that maintained the difference frequency  $\Delta f$ .

#### a Side View

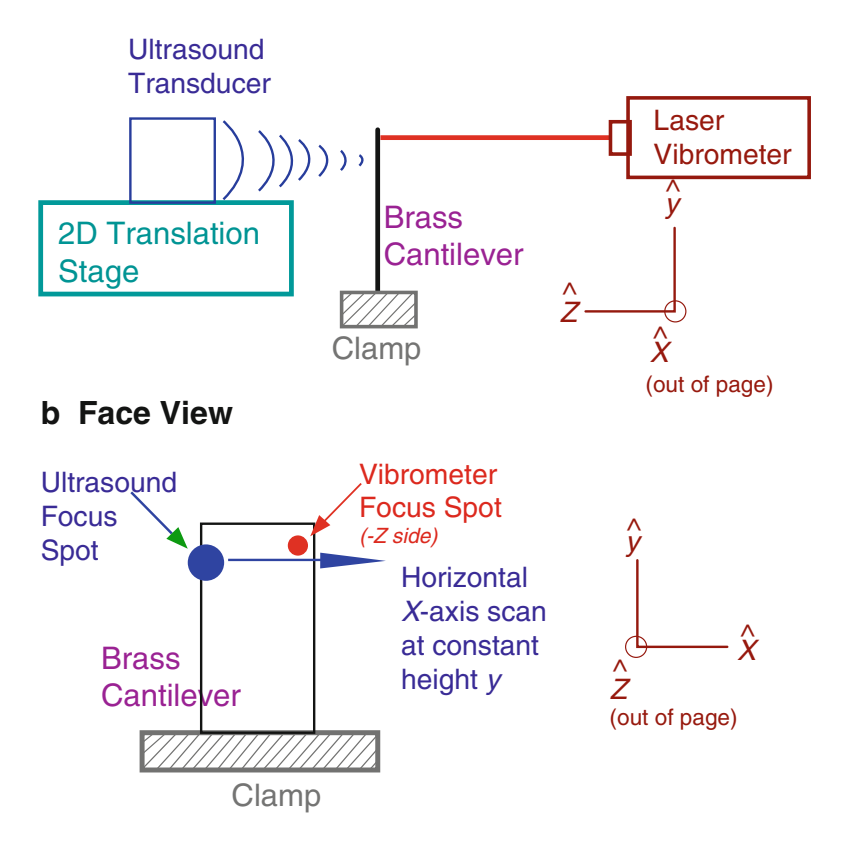


**Fig. 12.1** Schematic diagram of apparatus used for measuring edge-spread functions for ultrasound radiation force excitation. The ultrasound focus spot is moved horizontally across the width (*x*-axis) of the cantilever keeping the vertical position (*y*-axis) fixed. The vibrometer focus spot, used to measure the cantilever response, is fixed

### 12.2.2 Relationship Between Integrated Pressure And Acoustic Force Distributions

The goal of the current experiment was to correlate acoustic pressure distributions with acoustic radiation force measurements. Section 12.3 describes how a focused transducer was directed at the surface of a clamped-free cantilever. As shown in Fig. 12.1, the transducer was translated to multiple locations along the x-axis, ranging from positions where the ultrasound focus spot did not insonify the cantilever, to positions where the entire ultrasound focus spot was incident on the cantilever. For each x-position of the transducer, the acoustic radiation force was measured. In this case, the surface integral of Eq. (12.5) includes all x-values larger than x, and is called the edge-spread function ESF(x)

$$ESF(x) = k \int_{x'=x}^{+R} \int_{y'=-R}^{+R} dx' dy' P(f_1, x', y') P(f_2, x', y') .$$
 (12.6)

This definition of the edge-spread function is analogous to its usage in optics, where it is defined as the fraction of a circular beam pattern that passes by a sharp knife-edge surface [13]. In the current case, the sharp edge used to obtain the edge-spread function is the side of the cantilever. In the integral of Eq. (12.6), the limits of integration go to a value R. This is the effective maximum radius of the ultrasound focus spot; it is assumed that beyond this radius R, the ultrasound pressure is small enough that it would provide a negligible contribution to the edge-spread function. The integral for the edge-spread function can be rewritten as

$$ESF(x) = \int_{x'=x}^{+R} LSF(x') dx'$$
(12.7)

where LSF(x') is called the line-spread function, and is given by

$$LSF(x') dx' = k \left[ \int_{y'=-R}^{+R} P(f_1, x', y') P(f_2, x', y') dy' \right] dx'.$$
 (12.8)

Physically, the line-spread function can be considered as the acoustic radiation force that results from a narrow strip of the ultrasound distribution along the y-axis that is located at position x'. As will be discussed in Sect. 12.4.2, for the current experiment, the pressure distribution at frequencies  $f_1$  and  $f_2$  were nearly identical. This means that the integrand of Eq. (12.8) can be replaced by the square of the pressure at the central frequency  $f_C$ , in other words

$$LSF(x') dx' = k \left[ \int_{y'=-R}^{+R} P(f_c, x', y')^2 dy' \right] dx'.$$
 (12.9)

From Eq. (12.7), it is clear that another method for determining the line-spread function is to take the numerical derivative of a measured edge-spread function [13]

$$LSF\left(x'\right) = \frac{d}{dx}\Big|_{x=x'} ESF(x). \tag{12.10}$$

### 12.2.3 Numerical Differentiation Using Low-Noise Lanczos Technique

As described in Sect. 12.4.3, the line-spread function was obtained by taking the numerical derivative of the measured edge-spread function. Because of random noise in the edge-spread function, a simple two-point technique leads to large fluctuations in the numerical derivative. Therefore, it is helpful to employ a multi-point numerical differentiation technique. One such algorithm is the low-noise Lanczos algorithm [14]. One of the advantages of this technique is that it is symmetric around a central point and it is efficient at smoothing random noise [15]. For a data set with y-values  $f_k$  discretely sampled with a uniform x-axis spacing of h, the Lanczos N-point numerical estimate of the derivative at x' is determined by

$$\left. \frac{df}{dx} \right|_{x=x'} \approx \frac{3}{h} \sum_{k=1}^{m} k \frac{f_k - f_{-k}}{m(m+1)(2m+1)}, \quad \text{where} \quad m = \frac{N-1}{2}.$$
 (12.11)

# 12.3 Experimental Setup and Procedure

Figure 12.1 shows schematically the apparatus used in the current experiment. The cantilever was a strip of brass with dimensions of 19.6 by 8.1 by 0.37 mm clamped at one end in a machinist's vise. The vise had a mass of about 2 kg and was bolted to a Newport optical vibration isolation table to make a stable support. The resonance frequency of the lowest operating deflection shape of this cantilever was  $610 \pm 2$  Hz and corresponds to the 1st bending mode.

The BAT6 transducer used was a custom-made ultrasound transducer for operation in air (MicroAcoustic Instruments, Gatineau, Quebec, Canada). This transducer has a focal length of 70 mm and produces a focused ultrasound spot with a beam profile roughly 2.5 mm in diameter. The transducer had a central maximum located near 700 kHz with a bandwidth of over 200 kHz. Measurements by the manufacturer indicated that the pressure field produced by the BAT6 transducer was circularly symmetric at the focal point. Namely, the pressure amplitude at any radius r from the center of the distribution was essentially independent of the angle. The manufacturer provided a data set for the radial pressure distribution function P(r) at a distance of 76 mm from the surface of the transducer; this radial pressure distribution was measured by scanning a 250  $\mu$ m measurement transducer across the BAT6 transducer's focal spot.

In the current experiment, the BAT6 transducer was attached to an orthogonal pair of Newport 423 translation stages with computer-controlled Zaber Technologies T-NA08A25 micrometers with 0.05 μm resolution and 25.4 mm travel. Thus, the

location of the transducer focus point could be raster scanned over a range of positions, including points that were beyond the edges of the cantilever.

The transducer's waveforms were output from a 4-channel Strategic Test UF2e-6022 60 MSamples/Second Arbitrary Waveform Generator PCI express board (Stockholm, Sweden). This board generated the Double-Sideband, Suppressed Carrier (DSB-SC) waveform of Eq. (12.1) with a carrier frequency in the vicinity of 600 kHz, and a pair of sidebands separated by 610 Hz. This waveform was amplified using an ENI-240L RF amplifier to about 250Vpp. Another DAC output channel continuously cycled a simple 610 Hz sine wave that was used as a reference signal.

To determine the vibration of the cantilever, a Polytec PSV-400 Scanning Laser Doppler Vibrometer (Waldbronn, Germany) was focused near the free end of the cantilever. The vibrometer analog output signal was routed into a Zurich Instruments HF2LI Lock-In Amplifier (Zurich, Switzerland) with the reference signal being the 610 Hz sine wave produced by the Strategic Test card.

#### 12.4 Results

# 12.4.1 Experimental Measurement of Edge-Spread Function of BAT6 Ultrasound Transducer

For a point source applied to a clamped-free cantilever near its free end, simple Euler-Bernoulli beam theory predicts that fundamental mode response of the cantilever is independent of horizontal position [11]. For the current experiment, this was demonstrated using a reciprocal approach [16]. The ultrasound transducer was driven using a DSB-SC waveform with a carrier frequency near 600 kHz that had a difference frequency equal to the 610 Hz resonance frequency of the fundamental mode of the cantilever. With this fixed excitation transducer, the scanning vibrometer beam measured the vibration along a horizontal slice where the y axis position was fixed. For a y location within about 10 mm of the free end of the cantilever, the amplitude of vibration for any of these horizontal slices varied by less than 3 % across from width of the cantilever. By reciprocity this implies that for a roving point-source force, where a point-source was translated horizontally across the width of the cantilever, a fixed-location vibrometer would measure essentially the same amplitude regardless of where the point-source was applied along the x axis.

The apparatus shown in Fig. 12.1 was used to demonstrate that a roving-transducer technique could be utilized to measure the edge-spread and line-spread functions for the ultrasound transducer. As discussed in Section 12.2, the ultrasound transducer produced a DSB-SC waveform that had a difference frequency of 610 Hz. The vibrometer beam was located at a fixed position on the cantilever, and was used to monitor the vibration of the cantilever at its 610 Hz resonance frequency. The ultrasound transducer was positioned about 5 mm below the free end of the cantilever along the *y*-axis. Using the computer-controlled translation stage system, the transducer was positioned at multiple locations along the horizontal *x*-axis. The vibrometer measured the cantilever response at 610 Hz for each transducer location. Figure 12.2 shows the normalized vibration amplitude for each transducer location; these were normalized by dividing each vibration amplitude by the maximum vibration amplitude. In this figure, the x = 0 point corresponds to the transducer being centered on one edge of the cantilever. For large negative *x* values, the transducer was directed to a location where it was not striking the cantilever, and for large positive *x* values, the entire focal spot was incident on the cantilever.

Theoretically, if the output of a transducer was focused to an infinitesimally small radius, in other words a point-source force, the response function of Fig. 12.2 would be a square edge that would rapidly go from 0 to 1. However, because of the finite size of the ultrasound focus spot, the distribution shown in Fig. 12.2 shows that the cantilever's response varies from 0 to 1 over a range of several mm centered on the edge of the cantilever. The edge-spread function for this transducer was measured by performing horizontal sweeps similar to Fig. 12.2 for both the left and right edges of the cantilever, with similar results. A previous study [17] demonstrated that by performing a vertical transducer scan, and fitting the resulting measured distribution to the deflection shape predicted by Euler-Bernoulli beam theory, the result was an edge-spread function that was nearly identical in shape to Fig. 12.2.

# 12.4.2 Determination of Line-Spread Function from Manufacturer-Measured Radial Pressure Distribution

A major goal of the current research study was to demonstrate the feasibility of using the measured edge-spread function of Fig. 12.2 to determine the line-spread function of the transducer. To verify this hypothesis, it was necessary to independently

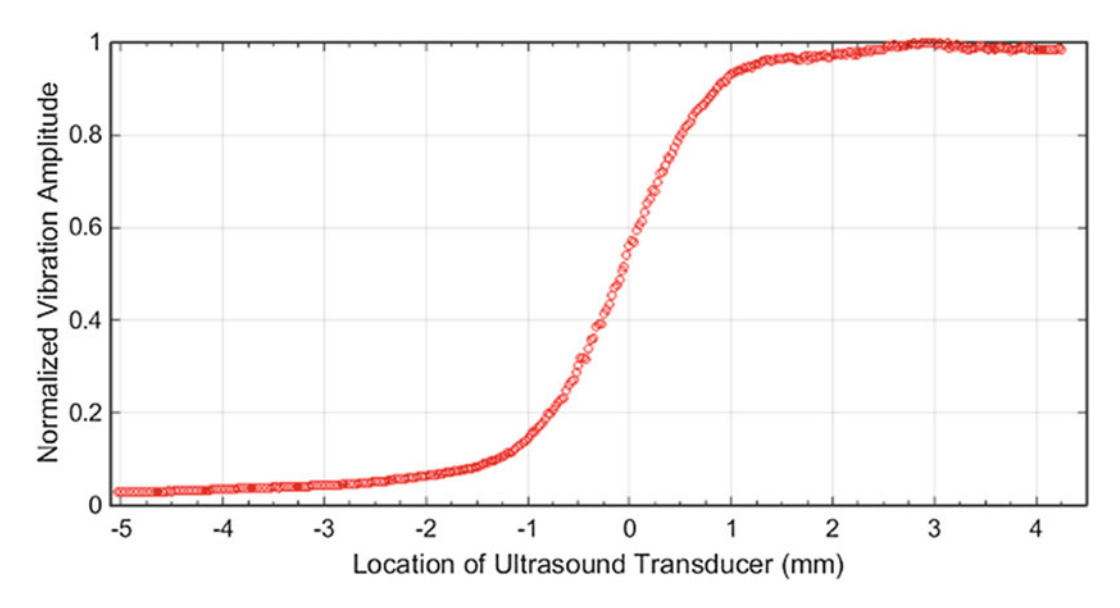


Fig. 12.2 Normalized response, also known as the edge-spread function, obtained when the ultrasound focus point was scanned across horizontal width of cantilever

determine the line-spread function. The line-spread function, defined by Eq. (12.9), was determined by integrating narrow strips of the 2-dimensional pressure distribution. The manufacturer provided a 1-d scan of the pressure distribution as a function of radius. Because the transducer's pressure distribution was circularly symmetric, the radial distribution could be rotated around the origin to obtain the 2-dimensional pressure distribution shown in Fig. 12.3. This pressure distribution was measured for a single frequency at 600 kHz with a focal depth of 76 mm. The central spot size for this pressure distribution was about 2.5 mm across. During the current study, a DSB-SC signal was used, where the carrier frequency was randomly varied within a range of 575 to 625 kHz. There would be pair of sidebands separated by 610 Hz for every carrier frequency. Based on measurements at other frequencies provided by the manufacturer, it was estimated that the width of the focal spot would vary by only about 0.1 mm for the range of frequencies used in the current experiment. Therefore, in the analysis that follows, the pressure distribution of Fig. 12.3 was used as representative for all frequencies used. This is constituent with the assumption that was made in deriving Eq. (12.9) where the acoustic radiation force was proportional to the square of the pressure distribution measured at a single frequency.

Figure 12.3 graphically illustrates the integral used for determining the line-spread function as a narrow black strip. The X's in Fig. 12.4 show the line-spread function obtained by taking integral of the square of the pressure, as in Eq. (12.9), for narrow strips of width dx' = 0.1 mm.

# 12.4.3 Determination of Line-Spread Function Using Numerical Differentiation of Edge-Spread Function

Determining of line-spread function, as described in Sect. 12.4.2, required knowledge of the pressure distribution, in this case furnished by the manufacturer. The goal of the current study was to demonstrate the feasibility of determining the line-spread function of the ultrasound transducer using a vibrometer. From Eq. (12.10), the numerical derivative of the measured edge-spread function (e.g. Fig. 12.2), was used to obtain the line-spread function. When a simple two-point derivative approximation was used, random noise caused rapid fluctuations in the numerical derivative. Therefore, the data set was differentiated using a multipoint method, in this case the low-noise Lanczos method of Eq. (12.11). Applying an N=9 point numerical differentiation technique resulted in the plot shown with open circles in Fig. 12.4. In experimenting with different values for the order parameter N, a tradeoff was observed: a large value of N led to a smoother curve with better noise reduction, but also meant a loss of other structure such as the shoulder expected in the vicinity of +/-2 mm. It was determined that an N=9 point derivative gave an acceptable tradeoff between smoothing noise without eliminating the structure of the distribution.

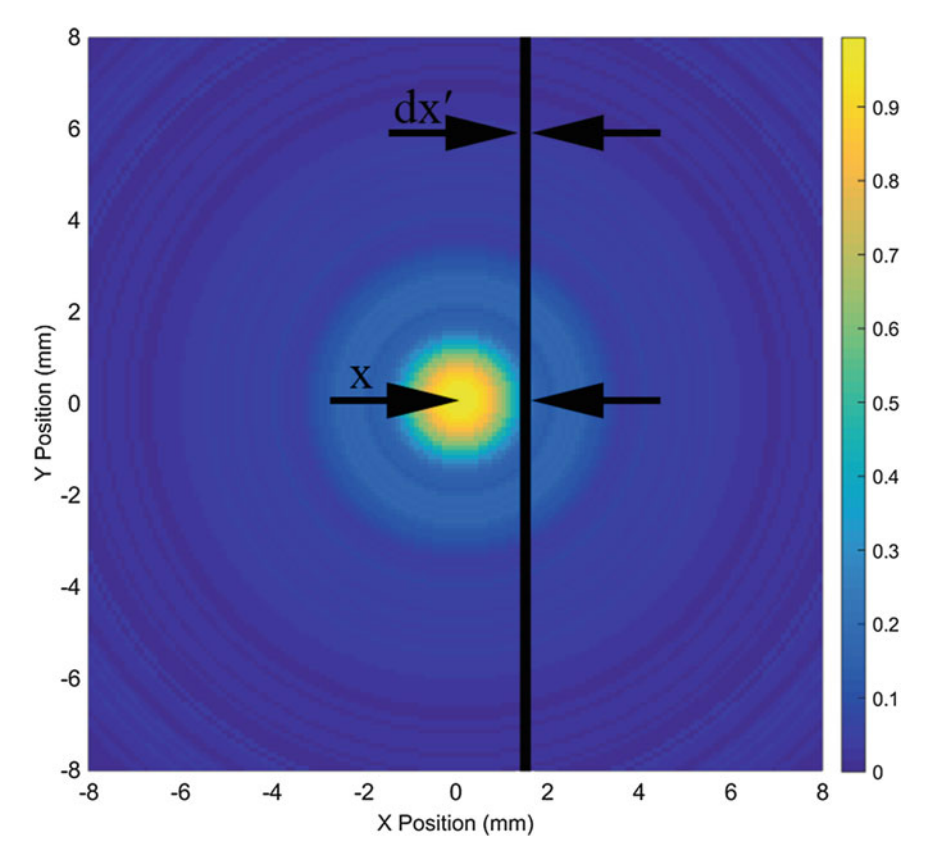


**Fig. 12.3** Two-dimensional ultrasound pressure distribution for BAT6 transducer used in the current experiment. This plot was obtained by rotating the radial pressure distribution, measured by the manufacturer, around the central focus point. The narrow *black line* illustrates the integral of Eq. (12.9) used to calculate the line-spread function

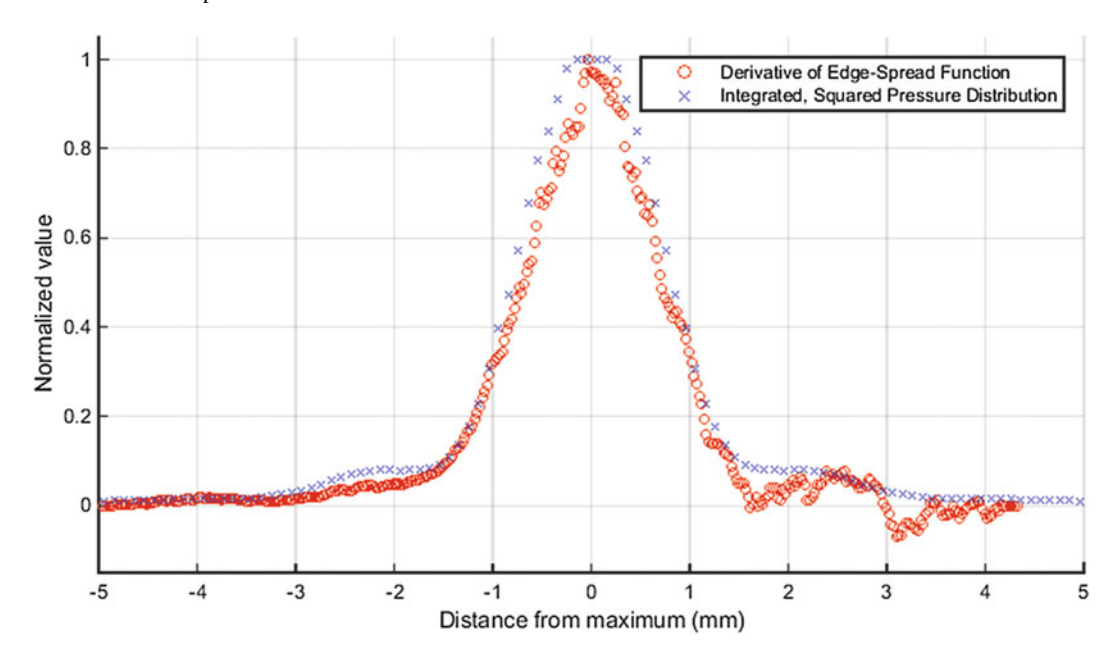


**Fig. 12.4** Comparison of line-spread functions for BAT6 ultrasound transducer. The measured edge-spread function of Fig. 12.2 was numerically differentiated to give the plot with *open circles*. The plot with X symbols is the integrated slice of the square of the pressure distribution (provided by the manufacturer). The agreement between these curves demonstrates the capability to extract an estimate of the line-spread function from an easily measurable edge-spread data set

#### 12.5 Conclusions

The current experiment demonstrates that it is possible to use the ultrasound radiation force of a roving transducer moving across a fixed-free cantilever to measure the edge-spread function of an ultrasound transducer. By taking the numerical derivative of this edge-spread function, the transducer's line-spread function could be determined. This is important because it is essential to know the spatial distribution, in particular the line-spread function, when modeling the radiation force applied to a structure.

In comparing the two plots in Fig. 12.4, there are some important conclusions. Most important, the line-spread function determined using a vibrometer and translation stage has a width and overall structure that is in good agreement with a line-spread function obtained by integration of pressure measurements. This vibrometer-measurement technique may be advantageous because many engineering labs have a single-point or scanning vibrometer, but might not have instrumentation needed to measure a radial pressure distribution directly. One major difference was the relatively large dips that occur at about 1.5 and 3.2 mm in the vibrometer measurement of line-spread function. These dips were due to some oscillations that are observed in the edge-spread function of Fig. 12.2, and will be investigated in more detail in future studies with different transducers.

Future studies will also involve utilizing the edge-spread function and line-spread function to determine the radial-distribution and 2-d distribution of the ultrasound radiation force applied by a transducer. One ultimate goal of this research program is determination of frequency response functions (FRF's) using a fully non-contact method for both excitation and measurement.

**Acknowledgements** The authors would like to thank David Schindel, President of Microacoustic Instruments, for measurement of the radial pressure distribution for this transducer. The authors would also like to thank Pete Avitabile and Chris Niezrecki of UMass-Lowell for valuable suggestions and discussion. This material is based upon work supported by the National Science Foundation under Grant Number 1300591. Any opinions, findings and conclusions or recommendations expressed in this material are those of the author(s) and do not necessarily reflect the views of the National Science Foundation (NSF).

#### References

- 1. Huber, T.M., Abell, B.C., Mellema, D.C., Spletzer, M., Raman, A.: Mode-selective noncontact excitation of microcantilevers and microcantilever arrays in air using the ultrasound radiation force. Appl. Phys. Lett. 97, 214101 (2010)
- 2. Huber, T.M., Beaver, N.M., Helps, J.R.: Noncontact modal excitation of a classical guitar using ultrasound radiation force excitation. Exp. Tech. 37(4), 38–46 (2013)
- 3. Huber, T.M., Fatemi, M., Kinnick, R., Greenleaf, J.: Noncontact modal analysis of a pipe organ reed using airborne ultrasound stimulated vibrometry. J. Acoust. Soc. Am. 119, 2476–2482 (2006)
- 4. Fatemi, M., Greenleaf, J.F.: Ultrasound-stimulated vibro-acoustic spectrography. Science 280, 82–85 (1998)
- 5. Silva, G.T., Chen, S.G., Greenleaf, J.F., Fatemi, M.: Dynamic ultrasound radiation force in fluids. Phys. Rev. E 71, 9 (2005)
- 6. Fatemi, M., Greenleaf, J.F: Acoustic force generation by amplitude modulating a sonic beam. US Patent 5,921,928, 1999
- 7. Fatemi, M., Greenleaf, J.F.: Mode excitation and imaging by the radiation force of ultrasound. J. Acoust. Soc. Am. 111, 2472 (2002)
- 8. Mitri, F.G., Trompette, P., Chapelon, J.Y.: Detection of object resonances by vibro-acoustography and numerical vibrational mode identification. J. Acoust. Soc. Am. 114, 2648–2653 (2003)
- 9. Huber, T.M., Calhoun, D., Fatemi, M., Kinnick, R. R., Greenleaf, J.F.: Noncontact modal testing of hard-drive suspensions using ultrasound radiation force. In: Proceedings of International Modal Analysis Conference XXIV, St Louis MO, February 2006
- 10. Westervelt, P.J.: The theory of steady forces caused by sound waves. J. Acoust. Soc. Am. 23, 312–315 (1951)
- 11. de Silva, C.W.: Euler-Bernoulli beam theory. In: Vibration: Fundamentals and Practice, pp. 346–351. CRC Press, Taylor & Francis Group, Boca Raton, FL (2007)
- 12. Huber, T.M., Beaver, N.M., Helps, J.R.: Elimination of standing wave effects in ultrasound radiation force excitation in air using random carrier frequency packets. J. Acoust. Soc. Am. 130(4), 1838–1843 (2011)
- 13. Optical transfer function. Wikipedia, the free encyclopedia. 02-Sep-2015
- 14. Lanczos, C.: Applied Analysis. Dover Books, New York, NY (1988)
- Holoborodko, P. Low-noise Lanczos differentiators. [Online]. Available: http://www.holoborodko.com/pavel/numerical-methods/numerical-derivative/lanczos-low-noise-differentiators/ Accessed 11 October 2015
- 16. Avitabile, P. Experimental modal analysis: A Simple Non-Mathematical Presentation. Sound Vib. Mag. 35, 1-15 (2001)
- 17. Huber, T.M., Batalden, S.M., Doebler, W.J.: Measurement of vibration resulting from non-contact ultrasound radiation force. In: Proceedings of International Modal Analysis Conference (IMAC-XXXIII), Orlando, FL 2015